Phytochemistry 150 (2018) 12–22

Contents lists available at ScienceDirect

Phytochemistry

journal homepage: www.elsevier.com/locate/phytochem

Discrimination of different geographic varieties of *Gymnema sylvestre*, an anti-sweet plant used for the treatment of type 2 diabetes

Ha Thanh Tung Pham [a, 1], Minh Chau Hoang [b, 1], Thi Kim Quy Ha [a], Lan Huong Dang [a], Van On Tran [c], Thi Bich Thu Nguyen [d], Chul Ho Lee [e], Won Keun Oh [a, *]

[a] Korea Bioactive Natural Material Bank, Research Institute of Pharmaceutical Sciences, College of Pharmacy, Seoul National University, Seoul, 151-742, Republic of Korea
[b] Nam Duoc Pharmaceutical Joint Stock Company, Hanoi, Viet Nam
[c] Hanoi University of Pharmacy, Hanoi, Viet Nam
[d] National Institute of Medicinal Materials, Hanoi, Viet Nam
[e] Laboratory Animal Resource Center, Korea Research Institute of Bioscience and Biotechnology, Republic of Korea

ARTICLE INFO

Article history:
Received 2 December 2017
Received in revised form
2 February 2018
Accepted 20 February 2018

Keywords:
Gymnema sylvestre
Asclepiadaceae
Geo-diversity
Morphology
Anatomy
ITS sequences
Gymnemoside
3β-glucuronide oleane-triterpene
Glucose uptake

ABSTRACT

Gymnema sylvestre (Retz.) R.Br. ex Sm. (Asclepiadaceae) is a well-known Ayurvedic anti-sweet plant for the treatment of type 2 diabetes mellitus. Although it was previously proposed that G. *sylvestre* exhibits chemical variation based on geography, most research on *G. sylvestre* has used material originating from India. Morphological and anatomical descriptions, ITS1-5.8S-ITS2 DNA sequencing, and acid hydrolysis analyses showed that *G. sylvestre* samples from Vietnam are distinguishable from those of Indian origin and thus suggest a dissimilarity among *G. sylvestre* samples with different geographic distributions. An LC-MS-guided strategy targeting 3β-glucuronide oleane-triterpenes in the Vietnamese *G. sylvestre* variety led to the isolation of four known compounds and nine previously undescribed compounds, named gymnemosides ND1-ND9. None of the isolated compounds were reported in the Indian sample, further supporting the geo-diversity of *G. sylvestre*. Three compounds, gymnemosides ND7-9, exerted significant stimulatory effects on the uptake of 2-NBDG in 3T3-L1 adipocyte cells and thus have potential as lead molecules for anti-diabetes agents.

1. Introduction

In recent years, a growing awareness of the relationship between functional foods and health has led to increased interest in the development of physiological functional plants due to their potential health benefits (Zhao et al., 2017). *Gymnema sylvestre* (Retz.) R.Br. ex Sm. (Asclepiadaceae) is a well-known medicinal plant with a long history of use in Ayurvedic traditional medicine and has been studied extensively for its effectiveness in the treatment of type 2 diabetes mellitus (T2DM) (Pothuraju et al., 2014). This plant has been used in formulations such as a simple tea brew, tea bags, beverages and confectioneries (Tiwari et al., 2014) and has also been applied in various food preparations for the regulation of sugar homeostasis and the control of obesity and blood cholesterol levels. *G. sylvestre* has been blended with wheat (*Triticum aestivum*), legumes, non-fat dry milk, vegetable oils and spices to formulate suitable dietary supplements or meal alternatives for non-insulin-dependent diabetes patients (Shobana et al., 2007).

Most studies of *G. sylvestre* have been performed using material from India, and its main active components are a group of gymnemic acids with a β-glucuronic acid at C-3 and a hydroxyl substitution at C-23 on an oleane triterpene-type aglycone (Pothuraju et al., 2014). These gymnemic acids have long been recognized for their role in selectively suppressing sweet taste sensations in humans (Warren and Pfaffmann, 1959) (Frank et al., 1992) (Gent et al., 1999). Kashima et al. recently suggested that the subjective sweet taste intensity was decreased among volunteers administered *G. sylvestre* compared with a control group and revealed the role of an extract of *G. sylvestre* in delaying postprandial gastrointestinal blood flow and gastric emptying, which might affect the

* Corresponding author.
E-mail address: wkoh1@snu.ac.kr (W.K. Oh).
[1] These authors contributed equally to this work.

https://doi.org/10.1016/j.phytochem.2018.02.013
0031-9422/

subsequent glycemic metabolism (Kashima et al., 2017).

An LC-MS analysis of extracts of *G. sylvestre* from different geographic distributions (India, Vietnam and China) subjected to acid hydrolysis revealed similarities in the LC patterns between samples from Vietnam and China but significant discrepancies with the samples of Indian origin. Specifically, gymnemagenin, a 23-hydroxyl triterpene aglycone, was found in the Indian sample but not in the Vietnamese and Chinese samples (Fig. S7, Supplementary data). This result is consistent with the proposed chemical variation in *G. sylvestre* varieties from China, which are characterized by the absence of a 23-hydroxyl functional group in their oleanane-type triterpene glycosides (Ye et al., 2001b). Variations in the chemical composition of a medicinal plant can influence its pharmacological activity, safety and standardization. Thus, in this study, we investigated the discrimination of two varieties of *G. sylvestre* using different approaches, including morphological and anatomical analyses and ITS1-5.8S-ITS2 DNA sequence comparisons. Furthermore, an isolation process targeting 3β-glucuronide oleanane-triterpenes from *G. sylvestre* collected from Vietnam was performed and resulted in the purification and elucidation of nine previously undescribed compounds, named gymnemosides ND1-ND9 (**1**–**9**), and four known compounds (**10**–**13**). All the isolates were evaluated to assess their effect on glucose uptake in differentiated 3T3-L1 adipocyte cells using 2-NBDG as a fluorescent-tagged glucose probe with the aim of identifying the potential of the Vietnamese *G. sylvestre* variety for the treatment of T2DM.

2. Results and discussion

2.1. Morphological and anatomical analysis of two Gymnema sylvestre varieties

Detailed descriptions of the macroscopic and microscopic characteristics of two samples, Vietnamese *G. sylvestre* variety (GS-V) and Indian *G. sylvestre* variety (GS-I), revealed many similar morphological traits matching those of *G. sylvestre* (Retz.) R.Br. ex Sm., described in Flora of China (Wu and Raven, 1995) (Figs. S1 and S2, Supplementary data). Despite these similarities, some distinctive characteristics could be used to differentiate the two samples (Fig. 1A): (1) young branchlets that were glabrescent or pubescent in GS-V but densely pubescent in GS-I; (2) leaf blades were diverse and varied from obovate to ovate in both samples but were more likely to be obovate and thickly papery in GS-V but obovate and thinner in GS-I; (3) adaxial and abaxial leaves that were nearly glabrous and slightly pubescent at the mid-vein in GS-V but pubescent at the midvein in GS-I; (4) four to five pairs of lateral veins in GS-V, in contrast to three to four pairs in the venation system of GS-I, with three more prominent veins converging at the base; and (5) follicle fruits that were broadly lanceolate with an acuminated beak on top in GS-V but smaller fruits with a narrowly lanceolate shape and no beak in GS-I (see Fig. 2).

To confirm the scientific names of these two samples, we further compared their morphological characteristics with TYPE specimens of *G. sylvestre* deposited at the Museum National d'Histoire Naturelle, Paris, France. The GS-V sample was similar to the HOLOTYPE specimen MNHN-P-P04256786 collected in Tonkin, Vietnam (Fig. S3, Supplementary data), whereas the GS-I sample was comparable to the "TYPE" specimen MNHN-P-P00645841 from India (Fig. S4, Supplementary data). Another SYNTYPE specimen, MNHN-P-P00442712 (Fig. S5, Supplementary data) from Madagascar (Africa), also matched GS-I. All type specimens mentioned above were identified as *G. sylvestre*. Although the two studied samples were determined to be the same species, their differences were sufficiently obvious, indicating that the samples represent two different varieties of *G. sylvestre* (Retz.) R.Br. ex Sm.

2.2. ITS1-5.8S-ITS2 sequence analysis of different Gymnema accessions

The ITS region encompasses two noncoding regions, ITS1 and ITS2, separated by the highly conserved 5.8S rRNA gene (White et al., 1990). A multiple alignment analysis of 21 samples also illustrated the conservation of the 5.8S region, with only two single nucleotide polymorphisms (SNPs). Variations between samples mainly occurred in the ITS1 and ITS2 regions (Fig. S6-A, Supplementary data), promising significant separation among closely related species. Accordingly, the neighbor-joining phylogenetic tree showed clear divisions among all the samples at the inter-species level, with pairwise genetic distances based on identity that varied from 90.9% (between the *G. sylvestre* Indian variety and *G. latifolium*) to 96.4% (between the *G. sylvestre* Vietnamese variety and *G. yunnanense*) (Fig. S6-B, Supplementary data). At the intra-species level, the *G. sylvestre* samples were divided into two groups (Fig. 1B) that strongly referred to the native origins of Vietnam and India. The molecular differences between the two groups of *G. sylvestre* samples were consistent with the morphological analysis and further supported the discrimination of the two varieties.

2.3. Isolation and structural elucidation of compounds from the Vietnamese Gymnema sylvestre variety

Through LC-MS in the positive mass fragmentation mode, 3β-glucuronide oleane-triterpenes can be effectively discriminated from other triterpenes in *G. sylvestre* based on a neutral loss of 176 Da (corresponding to glucuronic acid). Thus, an LC-MS-guided strategy was used to isolate the target glucuronide triterpenes from *G. sylvestre* with the following procedure: (1) extraction of *G. sylvestre* leaves with 60% EtOH under ultrasonic conditions; (2) column chromatography (CC)-based separation using macroporous resin; (3) open silica gel CC to obtain the enriched triterpenoid fraction; (4) purification using RP-18 (CC), Sephadex LH-20 (CC) and semi-preparative HPLC in a successive manner; and (5) structural elucidation by MS, NMR and acid hydrolysis/HPLC analysis. As a result, nine previously undescribed compounds, named gymnemoside ND1-ND9 (**1**–**9**), and four known compounds (**10**–**13**) were identified.

Gymnemoside ND1 **(1),** obtained as an amorphous powder with α_D^{25} -24.5^0 (*c* 0.2, MeOH), has the molecular formula $C_{42}H_{66}O_{16}$, as determined by the deprotonated molecular ion peak at *m/z* 825.4315[M−H]$^-$ (calcd for $C_{42}H_{65}O_{16}$, 825.4278), and 10 indices of hydrogen deficiency. The IR spectrum showed strong absorptions at 3399, 2943 and 1706 cm^{-1}, indicating the presence of hydroxyl and carbonyl functionalities. In the ^{1}H NMR spectrum, six methyl singlets at δ_H 0.81, 0.97, 0.99, 1.26, 1.38 and 1.58 (each 3H, s) were observed. Furthermore, one olefinic proton signal at δ_H 5.31 (1H, br s) and two anomeric protons at δ_H 4.98 (d, J = 7.5 Hz) and δ_H 5.37 (d, J = 8.0 Hz) were apparent. The ^{13}C NMR spectrum showed signals for 42 carbons, including two carboxyl groups at δ_C 181.6 and 172.5, two olefinic carbon signals at δ_C 143.6 and 123.5, two anomeric carbons at δ_C 107.0 and 106.1, and 11 oxygenated carbons in the range from δ_C 62.7 to 89.3. The above spectroscopic data suggested that **1** is an oleane-type triterpene with two sugar moieties (Yoshikawa et al., 1998). The carboxylic acid at δ_C 181.6 was assigned to C-29 through its HMBC correlations with H-30 (δ_H 1.58), H-19 (δ_H 2.70), and H-21 (δ_H 2.52). Through a comparison to the literature and an HMBC analysis, the oxygenated methylene protons at δ_H 4.41 (d, J = 10.3 Hz) and δ_H 3.75 (d, J = 10.3 Hz) were attached to C-28 (δ_C 68.2), and the oxygenated methine proton at δ_H 4.81 (dd, J = 12.0, 4.9 Hz) was posited at C-16 (δ_C 67.0) (Ye et al., 2000). The relative configuration of the aglycone was analyzed

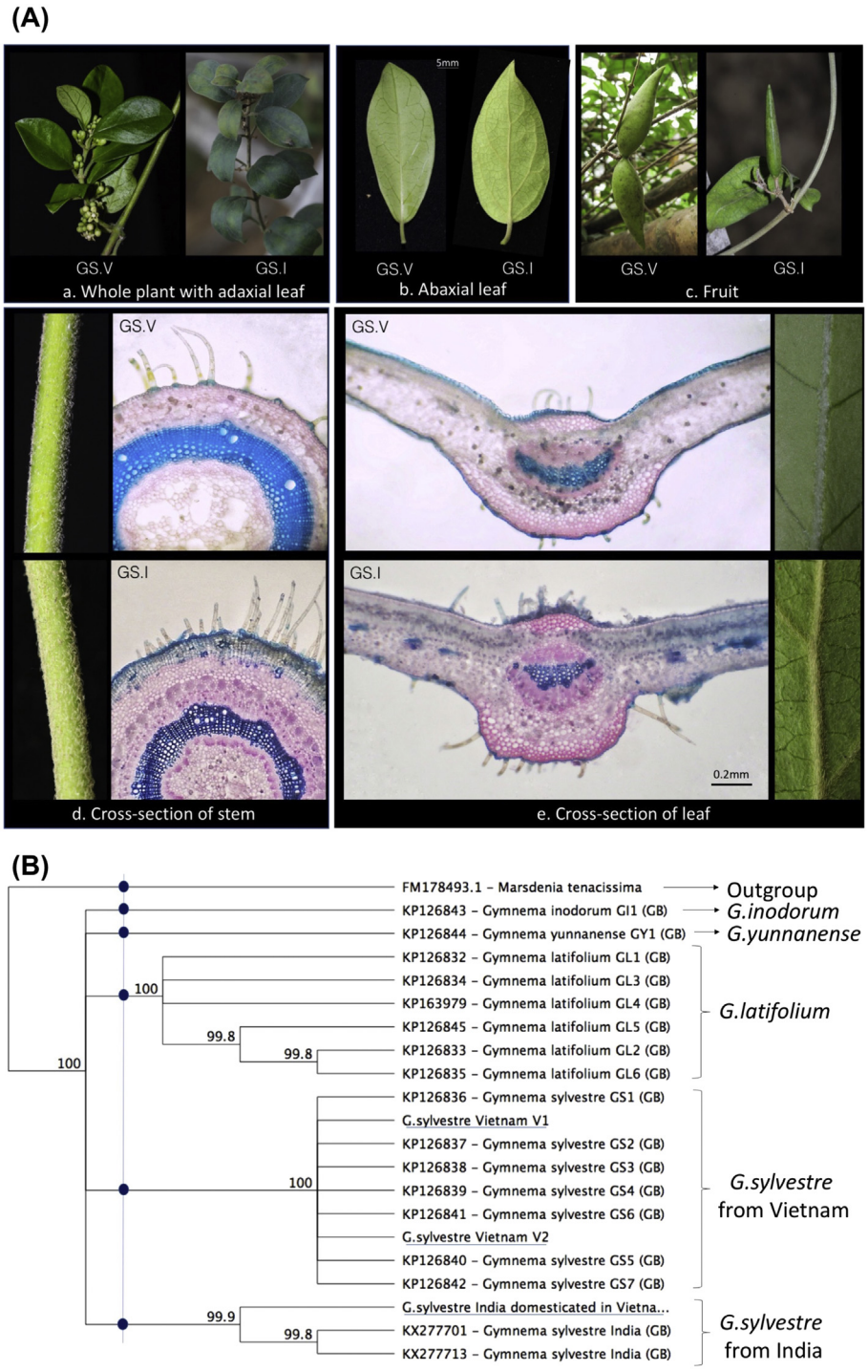

Fig. 1. A. Selective morphological and anatomical characteristics differentiating two varieties of *Gymnema sylvestre*. B. Neighbor-joining phylogenetic tree based on ribosomal internal transcribed spacer (ITS) sequences of different samples in the genus *Gymnema*. Bootstrap values expressed as percentages of 1000 replications (>75%) are shown above the branches. The underlined samples were directly sequenced in this study, and the other sample sequences were obtained from GenBank via Blast analysis. *Marsdenia tenacissima* was used as an outgroup sample for this study.

via proton coupling patterns and a NOESY experiment. The NOESY correlations from H-3 δ_H 3.32 (dd, $J = 11.5, 4.0$ Hz) to H-5 δ_H 0.74 (d, $J = 11.7$ Hz) indicated that OH-3 was found in a β orientation. NOESY cross peaks between H-27 δ_H 1.38 (3H, s) and H-16 δ_H 4.81 (dd, $J = 12.0$, 4.9 Hz) showed that OH-16 was projected in a β orientation. In addition, NOESY correlations between H-30 (3H, s) and H-18 δ_H 2.61 (dd, $J = 13.8, 3.9$ Hz) afforded the construction of the α equatorial conformation of Me-29. Therefore, the aglycone of **1** was deduced to be 3β-16β-28-trihydroxyolean-12-en-29-oic acid or myrtillogenic acid.

The acid hydrolysis of **1** yielded a mixture of sugars, which were identified as D-glucose and D-glucuronic acid through a comparison with authentic sugar standards. Their presence was supported by the positive mass fragment ions 629 [M-2 × H_2O-162 (glucose)+

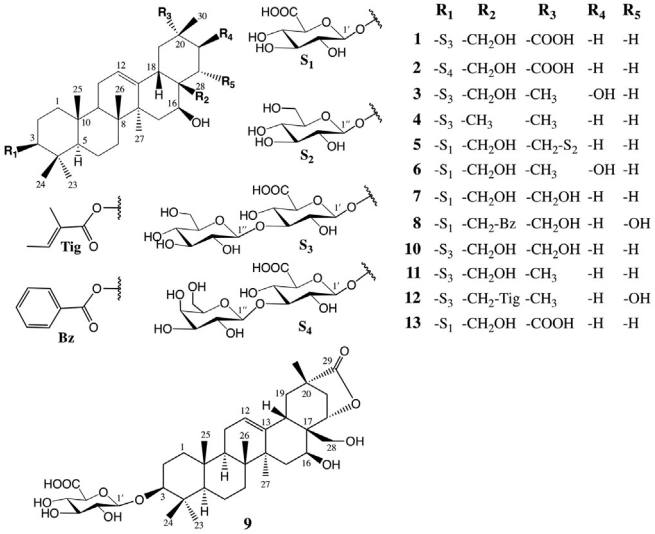

	R_1	R_2	R_3	R_4	R_5
1	-S_3	-CH_2OH	-COOH	-H	-H
2	-S_4	-CH_2OH	-COOH	-H	-H
3	-S_3	-CH_2OH	-CH_3	-OH	-H
4	-S_3	-CH_3	-CH_3	-H	-H
5	-S_1	-CH_2OH	-CH_2-S_2	-H	-H
6	-S_1	-CH_2OH	-CH_3	-OH	-H
7	-S_1	-CH_2OH	-CH_2OH	-H	-H
8	-S_1	-CH_2-Bz	-CH_2OH	-H	-OH
10	-S_3	-CH_2OH	-CH_2OH	-H	-H
11	-S_3	-CH_2OH	-CH_3	-H	-H
12	-S_3	-CH_2-Tig	-CH_3	-H	-OH
13	-S_1	-CH_2OH	-COOH	-H	-H

Fig. 2. Chemical structures of 13 compounds isolated from the Vietnamese *Gymnema sylvestre variety.*

H]$^+$ and 453 [M-2 × H_2O-162-176 (glucuronic acid)+H]$^+$ and two different series of hexose proton signals observed in the COSY spectrum. In the first sugar moiety, the proton at δ_H 4.98 (d, $J = 7.5$ Hz) was clearly the anomeric proton, and its coupling constant suggested that this glycoside moiety existed in β-isomer form. This sugar portion was suggested to be a β-glucuronic acid by the HMBC correlation from proton H-5′ δ_H 4.63 (d, $J = 9.5$ Hz) to carboxylic acid C-6′ (δ_C 172.5). The doublet signal ($J = 8.0$ Hz) of the anomeric proton H-1″ (δ_H 5.37 ppm) and the presence of two oxygenated methylene protons attached to C-6″ (δ_C 62.7) revealed a β-glucopyranosyl substitution. Further investigation of the HMBC spectra showed cross peaks between Glu-H1″ (δ_H 5.37) and GluA-C3′ (δ_C 87.8) and Glu-H1′ (δ_H 4.97) with the aglycone at C-3 (δ_C 89.3), supporting the linkage of the sugar moieties. Therefore, compound **1** was elucidated as 3β,16β,28-trihydroxyolean-12-en-29-oic acid 3-O-β-D-glucopyranosyl(1 → 3)-*O*-β-D-glucuronopyranoside.

Gymnemoside ND2 (**2**) was obtained as an amorphous powder with α_D^{25} -23.3^0 (*c* 0.2, MeOH). Its molecular formula was determined as $C_{42}H_{66}O_{16}$ based on HRESIMS ion peaks at *m/z* 825.4297 [M−H]$^-$ (calcd for $C_{42}H_{65}O_{16}$ 825.4278). The acid hydrolysis of **2** also yielded a mixture of sugars identified as D-galactose and D-glucuronic acid. ^{1}H and ^{13}C spectroscopic data for the aglycone of **2** (Tables 1 and 2) revealed signals identical to those of **1** with the exception a slight change in the chemical shifts of 3-*O*-β-D-glucose, which matched the chemical shifts of 3-*O*-β-D-galactose. Therefore, compound **2** was elucidated as a glycosidic isomer of **1**, 3β,16β,28-trihydroxyolean-12-en-29-oic acid 3-O-β-D-galactopyranosyl(1 → 3)-*O*-β-D-glucuronopyranoside.

Compound **13** was obtained as an amorphous powder with α_D^{25} -17.6^0 (*c* 0.2, MeOH), and its molecular formula of $C_{36}H_{56}O_{11}$ was determined by HRESIMS ion peaks at *m/z* 663.3778 [M−H]$^-$ (calcd for $C_{36}H_{55}O_{11}$ 663.3750). A comparison of the ^{13}C NMR data for compound **13** with those of gymnemic acid A (Wang et al., 2004) revealed similar chemical shifts, with the exception of the resonance of C-20, which was δ_C 43.1 in compound **13** but reported to be δ_C 28.5 in gymnemic acid A (Table S2, Supplementary data). To confirm the structure of **13**, we conducted an HMBC experiment and clearly identified correlations from H-30 (3H, s, δ_H 1.59), H-19 (δ_H 1.82, 1.71), and H-21(δ_H 2.52, 1.93) to C-20 (δ_C 43.1). Because the NMR chemical shift at C-20 of compound **13** also resembled that of compound **1** and ezoukoginoside A (Ge et al., 2016), the NMR data of gymnemic acid A were revised to those of compound **13** (Table S2, Supplementary data).

Gymnemoside ND3 (**3**) was obtained as an amorphous powder with α_D^{25} -5.9^0 (*c* 0.2, MeOH). Its molecular formula of $C_{42}H_{68}O_{15}$ was determined by a quasimolecular ion peak at *m/z* 811.4521 [M−H]$^-$ (calcd for $C_{42}H_{67}O_{15}$ 811.4485) in HRESIMS. ^{1}H, ^{13}C, and HSQC NMR spectroscopic data for the aglycone (Tables 1 and 2) revealed signals for seven methyl groups, an olefinic group and four oxygenated carbons. These NMR data shared identical values with those of sitakisogenin (Yoshikawa et al., 1994), and HMBC correlations from Me-29, 30 (each 3H, s, δ_H 1.25) to C-19 (δ_C 47.9), C-20 (δ_C 37.1) and C-21 (δ_C 73.1) confirmed the hydroxy group substitution at C-21. The glycosylation chemical shift of C-3 (δ_C 89.4, +10.9 ppm) obtained through a comparison with sitakisogenin (Yoshikawa et al., 1994) and HMBC cross peaks from Glu-H1″ δ_H 5.36 (d, $J = 7.7$ Hz) to GluA-C3′ (δ_C 87.6), Glu-H1′ δ_H 4.95 (d, $J = 7.5$ Hz) to C-3 (δ_C 89.4) confirmed the structure and linkage of the sugar portion. Based on all these data, compound **3** was elucidated as sitakisogenin 3-*O*-β-D-glucopyranosyl (1 → 3)-*O*-β-D-glucuronopyranoside.

Gymnemoside ND4 (**4**), which was obtained as an amorphous powder with α_D^{25} -8.7^0 (*c* 0.2, MeOH), possesses a molecular formula of $C_{42}H_{68}O_{13}$, as determined through HRESIMS ion peaks at *m/z* 779.4625 [M−H]$^-$ (calcd for $C_{42}H_{67}O_{13}$ 779.4582). The ^{1}H-NMR spectrum of **4** showed eight tertiary methyl groups and 12 oxymethine protons. The signals in the ^{13}C NMR spectrum (Table 1) combined with the HSQC analysis results led to the assignment of eight quaternary carbons (one carboxylic acid at δ_C 172.5 and one olefinic at δ_C 145.3), 17 tertiary carbons (12 oxygenated methines and one olefinic carbon at δ_C 122.6), 10 secondary carbons (one oxygenated methylene at δ_C 64.8), and eight methyl carbons. These NMR resonances, together with the results of the NOESY experiment (Fig. 3), suggested that **4** had a maniladiol aglycone due to the presence of a double bond at C_{12}-C_{13}, the eight methyl groups of an oleane skeleton and one β-oriented hydroxyl group substituted at C-16 (δ_C 64.8, δ_H 4.57) (Quijano et al., 1998). The carbon signals obtained due to the sugar moieties of **4** were also superimposable on those of compound **1**, indicating that the glycoside composition and linkage pattern were the same. Therefore, compound **4** was elucidated as 3β,16β-dihydroxyolean-12-en-3-*O*-β-D-glucopyranosyl (1 → 3)-*O*-β-D-glucuronopyranoside.

Gymnemoside ND5 (**5**) was obtained as an amorphous powder with α_D^{25} -22.3^0 (*c* 0.2, MeOH) and possesses the molecular formula of $C_{42}H_{68}O_{15}$, as determined through HRESIMS ion peaks at *m/z* 811.4526 [M-H]$^-$ (calcd for $C_{42}H_{67}O_{15}$ 811.4485). ^{1}H, ^{13}C and HSQC NMR spectroscopic data for the aglycone (Tables 1 and 2) revealed signals for six methyl groups and an olefinic bond at $C_{12\text{-}13}$. Signals of four oxygenated carbons were observed at δ_C 67.2, 69.0, 82.0, and 89.2, and positive mass fragmentation of four hydroxyl substitutions was detected. These NMR resonances combined with the results of a NOESY experiment (Fig. 3) suggested that the aglycone of **5** is gymnemagenol, specifically, 3β,16β,28,29 tetrahydroxyolean-12-en (Ye et al., 2001a). The LC-MS experiment in the positive mode showed similar mass fragment patterns with **1,** and the downfield shift of C-3 (δ_C 89.2, +11.0 ppm) and C-29 (δ_C 82.0, +8 ppm) compared with the gymnemagenol data suggested two sugar moieties attached to the main aglycone at C-3 and C-29. The NMR data for the saccharide portion showed that one of these two sugars was identical to the glucuronic acid substitution at C-3 of longispinogenin 3-*O*-β-D-glucuronopyranoside (Ye et al., 2000). The connection of the second glucose to the aglycone gymnemagenol at C-29 was confirmed by the HMBC correlation from H-1″ δ_H 4.84 (d, $J = 7.8$ Hz) to C-29 δ_C 82.0 and the NOESY correlation from H-30 δ_H 1.21 (3H, s) to H-18 δ_H 2.44 (dd, $J = 13.7, 3.9$ Hz). Hence, compound **5**

Table 1
^{13}C NMR spectroscopic data (C_5D_5N) of new compounds **1**–**9**.

No	1[b]	2[a]	3[a]	4[b]	5[b]	6[c]	7[c]	8[d,c]	9[b]
1	38.8, CH_2	38.9, CH_2	38.9, CH_2	39.0, CH_2	39.1, CH_2	39.1, CH_2	39.1, CH_2	39.4, CH_2	39.0, CH_2
2	26.8, CH_2	26.9, CH_2	26.8, CH_2	26.9, CH_2	27.0, CH_2	27.0, CH_2	27.0, CH_2	27.1, CH_2	26.9, CH_2
3	89.3, CH	89.3, CH	89.4, CH	89.5, CH	89.2, CH	89.3, CH	89.3, CH	89.4, CH	89.2, CH
4	39.8, C	39.8, C	39.8, C	39.9, C	39.9, C	39.8, C	39.9, C	40.0, C	39.8, C
5	55.8, CH	55.8, CH	55.9, CH	55.9, CH	56.0, CH	56.0, CH	56.0, CH	56.0, CH	55.9, CH
6	18.6, CH_2	18.7, CH_2	18.6, CH_2	18.7, CH_2	18.8, CH_2	18.8, CH_2	18.7, CH_2	18.8, CH_2	18.6, CH_2
7	33.1, CH_2	33.2, CH_2	33.2, CH_2	33.3, CH_2	33.3, CH_2	33.3, CH_2	33.2, CH_2	33.3, CH_2	33.6, CH_2
8	40.4, C	40.4, C	40.3, C	40.5, C	40.5, C	40.4, C	40.4, C	40.8, C	39.9, C
9	47.2, CH	47.3, CH	47.3, CH	47.4, CH	47.4, CH	47.4, CH	47.4, CH	47.5, CH	47.2, CH
10	37.0, C	37.0, C	37.0, C	37.1, C	37.0, C	37.1, C	37.0, C	37.1, C	37.1, C
11	24.1, CH_2	24.1, CH_2	24.1, CH_2	24.2, CH_2	24.1, CH_2	24.2, CH_2	24.1, CH_2	24.3, CH_2	24.0, CH_2
12	123.5, CH	123.1, CH	123.3, CH	122.6, CH	123.0, CH	123.4, CH	123.0, CH	123.8, CH	125.5, CH
13	143.6, C	143.7, C	143.4, C	145.3, C	144.1, C	143.5, C	144.4, C	142.6, C	140.1, C
14	44.0, C	44.1, C	44.0, C	44.3, C	43.9, C	44.2, C	44.2, C	43.0, C	44.4, C
15	36.9, CH_2	36.9, CH_2	36.9, CH_2	36.8, CH_2	37.0, CH_2	37.0, CH_2	37.1, C	36.6, CH_2	35.5, CH_2
16	67.0, CH	67.0, CH	67.9, CH	64.8, CH	67.2, CH	68.0, CH	67.2, CH	66.9, CH	66.7, CH
17	41.4, C	41.5, C	43.9, C	38.3, C	41.8, C	44.1, C	41.8, C	45.3, C	44.0, C
18	43.6, CH	43.6, CH	44.0, CH	49.9, CH	44.1, CH	44.0 CH	44.2, CH	43.8, CH	40.4, CH
19	41.8, CH_2	41.8, CH_2	47.9, CH_2	47.5, CH_2	42.2, CH_2	48.0, CH_2	42.2, CH_2	41.1, CH_2	40.2, CH_2
20	43.0, C	43.1, C	37.1, C	31.4, C	36.1, C	37.2, C	37.2, C	38.2, C	39.8, C
21	29.7, CH_2	29.7, CH_2	73.1, CH	35.2, CH_2	29.6, CH_2	73.1, CH	29.3, CH_2	39.2, CH_2	35.7, CH_2
22	25.4, CH_2	25.5, CH_2	35.1, CH_2	31.6, CH_2	25.7, CH_2	35.3, CH_2	26.0, CH_2	60.1, CH	79.6, CH
23	17.2, CH_3	17.2, CH_3	17.2, CH_3	17.3, CH_3	17.3, CH_3	17.2, CH_3	17.2, CH_3	17.4, CH_3	17.3, CH_3
24	28.3, CH_3	28.3, CH_3	28.3, CH_3	28.4, CH_3	28.5, CH_3	28.5, CH_3	28.5, CH_3	28.6, CH_3	28.4, CH_3
25	15.9, CH_3	15.9, CH_3	15.9, CH_3	16.0, CH_3	16.0, CH_3	16.0, CH_3	16.0, CH_3	16.1, CH_3	16.0, CH_3
26	17.1, CH_3	17.1, CH_3	17.2, CH_3	17.4, CH_3	17.2, CH_3	17.3, CH_3	17.3, CH_3	17.6, CH_3	17.3, CH_3
27	27.3, CH_3	27.4, CH_3	27.3, CH_3	27.7, CH_3	27.4, CH_3	27.4, CH_3	27.4, CH_3	28.2, CH_3	25.5, CH_3
28	68.2, CH_2	68.2, CH_2	68.5, CH_2	22.8, CH_3	69.0, CH_2	68.6, CH_2	69.2, CH_2	63.8, CH_2	64.1, CH_2
29	181.6, COOH	181.6, COOH	18.2, CH_3	24.5, CH_3	82.0, CH_2	18.3, CH_3	74.3, CH_2	73.9, CH_2	183.4, CH_2
30	20.6, CH_3	20.6, CH_3	30.3, CH_3	33.9, CH_3	20.5, CH_3	30.4, CH_3	20.4, CH_3	21.4, CH_3	21.7, CH_3
1′	107.0, CH	107.0, CH	106.8, CH	107.1, CH	107.6, CH	107.6, CH	107.6, CH	107.6, CH	107.6, CH
2′	74.7, CH	74.5, CH	74.7, CH	74.7, CH	75.9, CH	75.8, CH	75.9, CH	76.0, CH	75.8, CH
3′	87.8, CH	88.0, CH	87.6, CH	87.9, CH	78.5, CH	78.5, CH	78.4, CH	78.6, CH	78.4, CH
4′	71.8, CH	72.1, CH	71.8, CH	71.9, CH	73.8, CH	73.8, CH	73.8, CH	73.9, CH	73.7, CH
5′	77.6, CH	77.6, CH	77.5, CH	77.8, CH	78.1, CH	78.1, CH	78.5, CH	78.3, CH	78.2, CH
6′	172.5, COOH	172.5, COOH	172.9, COOH	172.5, COOH	173.4, COOH	173.4, COOH	173.2, COOH	173.6, COOH	173.2, COOH
1″	106.1, CH	103.9, CH	105.9, CH	106.2, CH	105.9, CH				
2″	75.9, CH	73.1, CH	75.8, CH	76.0, CH	75.6, CH				
3″	78.5, CH	73.2, CH	78.4, CH	78.6, CH	79.0, CH				
4″	72.0, CH	69.3, CH	72.0, CH	72.0, CH	72.1, CH				
5″	79.0, CH	76.8, CH	78.9, CH	79.1, CH	78.9, CH				
6″	62.7, CH_2	63.0, CH_2	62.7, CH_2	62.8, CH_2	63.2, CH_2				

Measured by:
[a] NMR-125 MHz.
[b] NMR-150 MHz.
[c] NMR-200 MHz.
[d] 28-*O*-benzoyl substitution: Bz-1 (δ_C167.3, C), Bz-2 (δ_C131.7, C), Bz-3,7 (δ_C130.2, CH), Bz-4,6 (δ_C129.5, CH), Bz-5 (δ_C133.8, CH).

was deduced as 29-*O*-(β-D-glucopyranosyl) gymnemagenol 3-*O*-β-D-glucuronopyranoside.

Gymnemoside ND6 (**6**) was obtained as an amorphous powder with α_D^{25} -15.7^0 (c 0.2, MeOH). Its molecular formula of $C_{36}H_{58}O_{10}$ was determined by HRESIMS ion peaks at m/z 649.3967 $[M-H]^-$ (calcd 649.3957). The ^{1}H and ^{13}C NMR spectroscopic data for **6** (Tables 1 and 2) showed resonances similar to those of **3** as well as a lack of resonance of a glucose unit, indicated by the shielded chemical shift of GluA-C3′. Accordingly, compound **6** was elucidated as sitakisogenin 3-*O*-β-D-glucuronopyranoside.

Gymnemoside ND7 (**7**), which was obtained as an amorphous powder with α_D^{25} -12.4^0 (*c* 0.2, MeOH), was found to possess the molecular formula of $C_{36}H_{58}O_{10}$ based on HRESIMS ion peaks at *m/z* 649.3985 $[M-H]^-$ (calcd 649.3957). LC-MS experiments in the positive mode, which showed a loss of 176 Da, and the pattern of the ^{13}C-NMR data for the sugar portion, which was superimposable with that of compound **6**, revealed the presence of a glucuronic acid substitution at C-3. The ^{1}H and ^{13}C NMR spectroscopic data for **7** (Tables 1 and 2) showed resonances similar to those of **5** and a lack of resonance of a glucose unit, as indicated by a shielded chemical shift of C-29 (δ_C 74.3, −7.7 ppm). Accordingly, compound **7** was identified as gymnemagenol-3-*O*-β-D-glucuronopyranoside.

Gymnemoside ND8 (**8**), obtained as an amorphous powder with α_D^{25} -2.4^0 (*c* 0.2, MeOH), possesses the molecular formula of $C_{43}H_{62}O_{12}$, as demonstrated by HRESIMS ion peaks at *m/z* 769.4210 $[M-H]^-$ (calcd 769.4169). The HPLC-MS results in the positive mode at 613 $[M-2\times H_2O-122+H]^+$ and 437 $[M-2\times H_2O-122-176+H]^+$ and the acid hydrolysis of **8** suggested the presence of glucuronic acid and benzoyl substitutions. ^{1}H, ^{13}C and HSQC NMR spectroscopic data for the aglycone (Tables 1 and 2) indicated six methyl groups, an olefinic group and five oxygenated carbons (δ_C 60.1, 63.8, 66.9, 73.9 and 89.4). The α equatorial conformation of OH-22 was identified through a comparison with the chemical shift of C-22 of alternoside X (Yoshikawa et al., 1998) and clear NOESY cross-peaks between H-22β (δ_H 4.98) and H-18β (δ_H 3.06). These NMR resonances identified the aglycone of **8** as 3β,16β,28,22α,29 pentahydroxyolean-12-en. The carbon signals due to the sugar moiety were superimposable on those of **6**, indicating glucuronic acid at C-3 (δ_C 89.4). The location of the benzoyl group on the triterpene skeleton was deduced by the HMBC correlations between

Table 2
^{1}H NMR spectroscopic data (C_5D_5N) of compounds **1**–**9**.

No	1[b]	2[a]	3[a]	4[b]	5[b]	6[c]	7[c]	8[d,c]	9[b]
1	1.42, overlap 0.89, t (7.5)	1.42, overlap 0.89, t (7.5)	1.38, overlap 0.83, overlap	1.42, overlap 0.89, t (7.5)	1.40, overlap 0.85, t (7.5)	1.38, overlap 0.83, overlap	1.40, overlap 0.85, t (7.5)	2.50, overlap 2.12, overlap	1.42, overlap 0.83, overlap
2	2.15, overlap 1.81, overlap	2.25, overlap 1.87, overlap	2.16, overlap 1.81, overlap	2.15, overlap 1.85, overlap	2.28, overlap 1.88, overlap	2.17, overlap 1.81, overlap	2.17, overlap 1.84, overlap	2.22, overlap 1.83, overlap	2.23, m 1.87, m
3	3.32, dd (4.0, 11.5)	3.36, dd (4.0, 11.5)	3.33, dd (11.5, 4.0)	3.36, dd (4.0, 11.5)	3.39, overlap	3.33, dd (11.5, 4.0)	3.37, dd (4.0, 11.5)	3.33, dd (9.9, 3.0)	3.36, dd (11.4, 3.2)
5	0.74, d (11.7)	0.74, d (11.7)	0.74, d (12.0)	0.74, d (11.7)	0.76, overlap	0.74, d (12.0)	0.76, d (11.7)	0.74, d (12.0)	0.71, d (11.4)
6	1.48, overlap 1.30, overlap	1.48, overlap 1.30, overlap	1.49, overlap 1.30, overlap	1.50, overlap 1.32, overlap	1.47, overlap 1.30, overlap	1.49, overlap 1.30, overlap	1.47, overlap 1.29, overlap	1.44, overlap 1.27, overlap	1.45, overlap 1.25, overlap
7	1.52, overlap 1.33, overlap	1.52, overlap 1.33, overlap	1.52, overlap 1.31, overlap	1.52, overlap 1.33, overlap	1.52, overlap 1.32, overlap	1.52, overlap 1.31, overlap	1.52, overlap 1.33, overlap	1.51, overlap 1.29, overlap	1.39, overlap 1.30, overlap
9	1.57, overlap	1.57, overlap	1.55, overlap	1.57, overlap	1.52, overlap	1.55, overlap	1.57, overlap	1.55, overlap	1.51, overlap
11	1.83, overlap 1.56, overlap	1.83, overlap 1.56, overlap	1.81, overlap 1.55, overlap	1.83, overlap 1.56, overlap	1.78, overlap	1.81, overlap 1.55, overlap	1.83, overlap 1.57, overlap	1.77, overlap 1.55, overlap	1.78, overlap
12	5.31, br s	5.31, br s	5.29, br s	5.30, br s	5.20, br s	5.29, br s	5.29, br s	5.36, br s	5.37, br s
15	2.24, t (13.0) 1.74, dd (12.0, 4.9)	2.25, t (13.0) 1.74, dd (13.0, 4.0)	2.22, t (13.0) 1.74, dd (13.0, 4.0)	2.07, t (13.0) 1.62, dd (13.0, 4.0)	2.24, t (13.0) 1.73, dd (13.0, 4.0)	2.22, t (13.0) 1.73, dd (13.0, 4.0)	2.25, overlap 1.76, dd (13.0, 4.0)	2.15, t (13.0) 1.71, dd (13.0, 4.0)	2.14, t (12.5) 1.61 (12.5, 4.3)
16	4.81, dd (12.0, 4.9)	4.81, dd (11.8, 4.9)	4.72, dd (11.3. 4.5)	4.57, overlap	4.67, overlap	4.72, dd (11.3. 4.5)	4.78, dd (13.0. 4.0)	5.29, dd (11.3. 5.2)	4.77, dd (12.5, 4.3)
18	2.61, dd (13.8, 3.9)	2.60, dd (13.7, 3.9)	2.58, dd (14.0, 4.0)	2.31, dd (13.8, 4.0)	2.44, dd (13.7, 3.9)	2.60, dd (14.0, 4.0)	2.52, overlap	3.06, dd (14.0, 5.6)	2.84, dd (12.5,8.9)
19	2.70, t (13.8) 1.79, dd (13.8, 3.9)	1.82, overlap 1.77, overlap	2.04, t (14.0) 1.45, overlap	1.90, overlap 1.15, overlap	2.08, overlap 1.35, overlap	2.04, t (14.0) 1.37, overlap	2.24, overlap 1.40, overlap	2.45, t (14.0) 1.38, overlap	2.10, t (12.5) 1.66 (12.5, 8.9)
21	2.52, td (13.5, 2.6) 1.93, overlap	2.52, td (13.3, 2.6) 1.93, overlap	4.18, overlap	2.07, overlap 1.63, overlap	1.93, overlap 1.47, td (13.3, 2.6)	4.14, overlap	2.05, overlap 1.48, dd (14.0, 3.5)	2.50, overlap 2.12, overlap	2.05, dd (12.0, 5.5) 2.67, d (12.0)
22	2.88, td (13.5, 2.6) 1.99, td (13.5, 2.6)	2.91, td (14.0, 2.6) 1.99, td (13.3, 2.6)	3.26, dd (13.5, 4.0) 2.07, t (13.5)	2.41, td (14.0, 2.6) 1.15, overlap	2.80, td (14.0, 2.6) 1.89, td (13.3, 2.6)	3.26, dd (13.5, 4.0) 2.06, t (13.5)	2.92, td (14.0, 3.5) 1.92, td (14.0, 3.5)	4.98, overlap	5.46, d (5.5)
23	0.97, s	0.98, s	0.96, s	1.00, s	1.00, s	0.97, s	1.02, s	0.96, s	0.99, s
24	1.26, s	1.26, s	1.27, s	1.30, s	1.31, s	1.27, s	1.29, s	1.28, s	1.28, s
25	0.81, s	0.82, s	0.79, s	0.86, s	0.83, s	0.79, s	0.83, s	0.79, s	0.81, s
26	0.99, s	0.99, s	0.96, s	1.03, s	1.00, s	0.97, s	1.00, s	1.10, s	0.87, s
27	1.38, s	1.38, s	1.36, s	1.39, s	1.33, s	1.37, s	1.39, s	1.44, s	1.22, s
28	4.41, d (10.3) 3.75, d (10.3)	4.42, d (10.3) 3.76, d (10.3)	4.37, d (10.5) 3.75, d (10.5)	1.15, s	4.41, d (10.3) 3.70, d (10.3)	4.39, d (10.5) 3.75, d (10.5)	4.47, d (10.3) 3.73, d (10.3)	5.44, d (10.5) 4.96, d (10.5)	4.45, d (10.5) 3.80, d (10.5)
29			1.25, s	0.98, s	3.92, d (8.3) 3.42, d (8.3)	1.25, s	3.60, 2H, overlap	3.65, dd (18.0, 10.0)	
30	1.58, s	1.59, s	1.25, s	0.93, s	1.21, s	1.25, s	1.22, s	1.33, s	1.27, s
1′	4.98, d (7.5)	4.95, d (8.0)	4.95, d (7.5)	5.00, d (7.7)	5.04, d (7.8)	5.02, d (7.7)	5.03, d (7.7)	5.00, d (7.7)	5.04, d (7.7)
2′	4.13, overlap	4.15, overlap	4.13, overlap	4.16, overlap	4.15, overlap	4.13, overlap	4.15, t (7.7)	4.13, t (7.7)	4.15, t (7.7)
3′	4.35, t (7.5)	4.29, t (8.0)	4.35, overlap	4.37, t (7.7)	4.35, t (7.8)	4.32, t (7.7)	4.35, t (7.7)	4.33, t (7.7)	4.36, t (7.7)
4′	4.51, overlap	4.55, overlap	4.52, overlap	4.55, overlap	4.61, overlap	4.58, t (7.7)	4.61, t (7.7)	4.59, t (7.7)	4.63, t (7.7)
5′	4.63, d (9.5)	4.64, d (9.5)	4.60, d (9.5)	4.65, d (9.0)	4.69, overlap	4.66, d (7.7)	4.69, d (7.7)	4.68, d (7.7)	4.71, d (7.7)
1″	5.37, d (8.0)	5.77, d (8.0)	5.36, d (7.5)	5.38, d (8.0)	4.84, d (7.8)				
2″	4.05, t (8.0)	4.01, t (8.0)	4.05, t (7.5)	4.07, t (8.0)	4.06, t (7.8)				
3″	4.23, t (8.0)	4.71, t (8.0)	4.22, t (7.5)	4.25, t (8.0)	4.24, overlap				
4″	4.17, overlap	4.19, overlap	4.13, overlap	4.18, overlap	4.24, overlap				
5″	4.02, overlap	4.56, overlap	4.01, overlap	4.02, overlap	3.98, t (7.8)				
6″	4.51, overlap 4.29, dd (10.9, 5.1)	4.50, overlap 4.30, dd (10.9, 5.1)	4.52, overlap 4.27, dd (10.9, 5.1)	4.53, overlap 4.31, dd (11.9, 5.9)	4.56, overlap 4.40, overlap				

Measured by:
[a] NMR-500 MHz.
[b] NMR-600 MHz.
[c] NMR-800 MHz.
[d] 28-*O*-benzoyl substitution: Bz-3,7 [each 1H, δ_H 8.27, (d, $J = 7.5$ Hz)], Bz-4,6 [each 1H, δ_H 7.43, (t, $J = 7.5$ Hz)], Bz-5 [1H, δ_H 7.51, (t, $J = 7.5$ Hz)].

H-28 [δ_H 5.44, d, $J = 10.5$ Hz]; δ_H 4.96, d, $J = 10.5$ Hz] and Bz-C-1″ (δ_C 167.3). These findings led to the assignment of **8** as 28-benzoyl-22α-hydroxygymnemagenol-3-*O*-β-D-glucuronopyranoside.

Gymnemoside ND9 (**9**), which was obtained as an amorphous powder with α_D^{25} -22.5^0 (c 0.2, MeOH), has the molecular formula of $C_{36}H_{54}O_{11}$, as determined by HRESIMS ion peaks at *m/z* 661.3616 $[M-H]^-$ (calcd for $C_{36}H_{53}O_{11}$ 661.3593). The HPLC-MS experiment results in the positive mode and the ^{13}C-NMR data for the sugar portion were superimposable on those of compound **6**. The linkage of glucuronic acid at C-3 was confirmed by anomeric proton signals [δ_H 5.04, (d, $J = 7.7$ Hz)] and the downfield shift of C-3 (δ_C 89.2). The remaining 30 carbon signals were assigned to an olean-12-ene skeleton as an aglycone based on the six singlet methyl protons, together with the typical olefinic carbon signals and one carboxylic carbon. The carboxylic was expected to form a γ-lactone ring with the hydroxyl group considering the degree of unsaturation and the presence of an esterified proton signal [δ_H 5.46, 1H, d ($J = 5.5$ Hz)]. The structure was fully elucidated through COSY, HSQC and HMBC spectra. The HMBC correlations of the methyl protons from H-30 (δ_H 1.27, 3H, s) to C-19 (δ_C 40.2), C-20 (δ_C 39.8), C-21 (δ_C 35.7) and C-

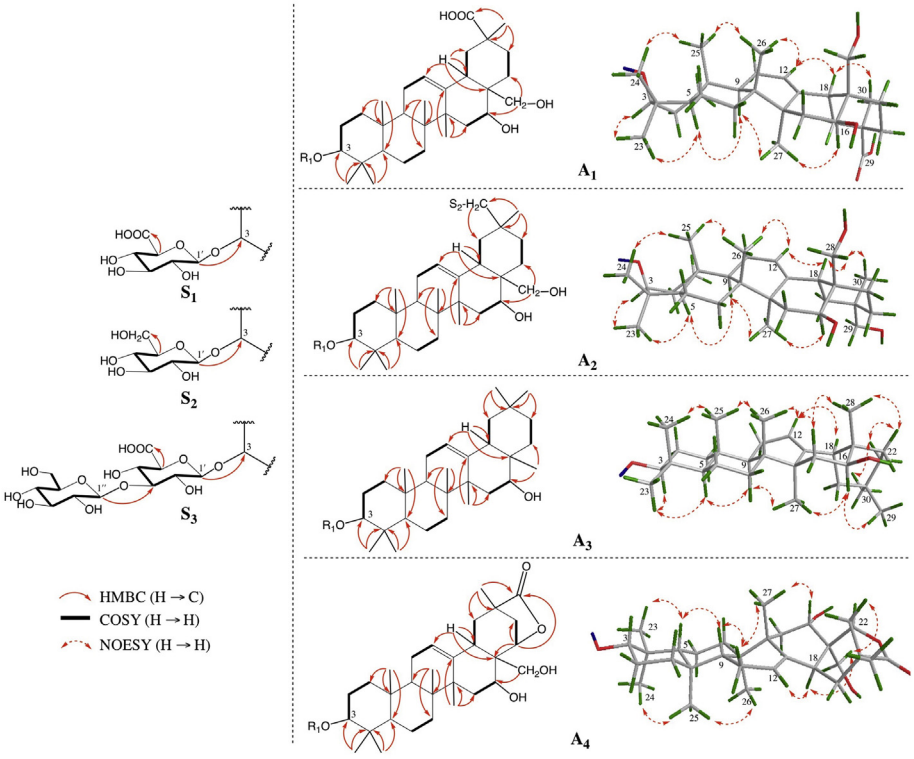

Fig. 3. $^{1}H-^{1}H$ COSY (▬), HMBC (⌒) and NOESY (⌒) correlations are shown as representative skeletons of the new compounds **1**–**9**. A1: myrtillogenic acid; A2: gymnemagenol, A3: maniladiol and A4: 3β,16β,28-trihydroxyolean-12-en-29,22β-olide.

29 (δ_C 183.4), from the esterified methine proton H-22 [δ_H 5.43, 1H, d ($J = 5.5$ Hz)] to C-18 (δ_C 40.4), C-28 (δ_C 64.1), and C-29 (δ_C 183.4), and from the carbinol proton H-28 (δ_H 4.45 and 3.80) to C-16 (δ_C 66.7) and C-22 (δ_C 79.6) revealed the structure of an aglycone, as shown in Fig. 3-A4. Moreover, NOE correlations between H-18β [δ_H 2.84 (1H, dd, $J = 12.5$, 8.9 Hz)], H-28β [δ_H 4.45 (1H, d, $J = 10.5$ Hz)] and H-22 [δ_H 5.46 (1H, d, $J = 5.5$ Hz)] suggested the stereochemistry of **9** shown in Fig. 3-A4. Thus, compound **9** was deduced as 3-*O*-β-D-glucuronopyranosyl-3β,16β,28-trihydroxyolean-12-en-29,22β-olide.

Based on the NMR, MS, and optical rotation data and a comparison with literature values, the known compounds were elucidated as 29-hydroxylongispinogenin 3-*O*-D-glucopyranosyl(1 → 3)-D-glucuronopyranoside (**10**) (Ye et al., 2001a), longispinogenin 3-*O*-D-glucopyranosyl(1 → 3)-D-glucuronopyranoside (**11**) (Ye et al., 2001a), alternoside XII (**12**) (Yoshikawa et al., 1999), and gymnemic acid A (**13**) (Wang et al., 2004). Notably, the NMR data for compound **13** were revised from the original published paper, and compounds **11** and **12** were found in free form for the first time, in contrast to the potassium salt form (M•K) reported for the same plant collected in the Guangxi Autonomous Region of China (Ye et al., 2001a). The HRMS chemical profiles of the 13 isolated compounds are illustrated in Fig. S8.

2.4. Effects of isolated compounds on glucose uptake in 3T3-L1 adipocyte cells

The compound 2-NBDG is a fluorescent glucose analog widely used for monitoring the uptake of glucose by cells and is a useful reagent for discovering insulin mimetic compounds (Lee et al., 2013). Here, we examined the stimulatory effects of compounds **1**–**13** on the uptake of 2-NBDG by 3T3-L1 adipocyte cells using an *in vitro* assay (2-NBDG assay) (Nguyen et al., 2017). 3T3-L1 fibroblasts were induced to differentiate into adipocytes. The isolated compounds were added at 20 μM to the differentiated 3T3-L1 adipocytes with 2-NBDG, with the exception of compounds **4**, **11** and **12**, which were added at 2 μM due to their observed dose-dependent cytotoxicity at concentrations of 5 and 10 μM (Fig. S64, Supplementary data). DMSO and insulin (0.1 μM) were used as negative and positive controls in this assay, respectively. As illustrated in Fig. 4A, compounds **5**–**10** significantly enhanced 2-NBDG uptake at 20 μM ($p < 0.05$). A detailed analysis of the structure-activity relationships (SARs) of all the isolates indicated that the 3-β-glucuronyl oleanane-type moiety might exert stimulatory effects on glucose uptake (compounds **5**–**9**). However, glycosylation of the aglycone or glucuronic acid clearly reduced the activities, particularly when glucose was attached to C-3′ of glucuronic acid (**7** > **5** > **10**). Additionally, the oxidation of the alcohol functional group at C-29 to a carboxylic acid markedly decreased the activity (**7** > **13**), and esterification of this carboxylic group recovered the activity (**9** > **13**).

Compared with insulin, compounds **7**–**9** showed the most potent stimulatory activities ($p < 0.01$). Further investigation revealed that the activities of compounds **7**–**9** on glucose uptake depended on the dose (Fig. 4B). To confirm the transportation efficacy of 2-NBDG into cells, we further measured the fluorescent signals in adipocytes after compound treatment through fluorescence microscopy (Fig. 4C and Fig. S65 - Supplementary data). As expected, compounds **7**–**9** (at a concentration of 10 μM) produced higher-intensity fluorescent signals in adipocytes compared with the control group (treated with DMSO), and these fluorescence intensities were as high as those obtained with insulin treatment (0.1 μM).

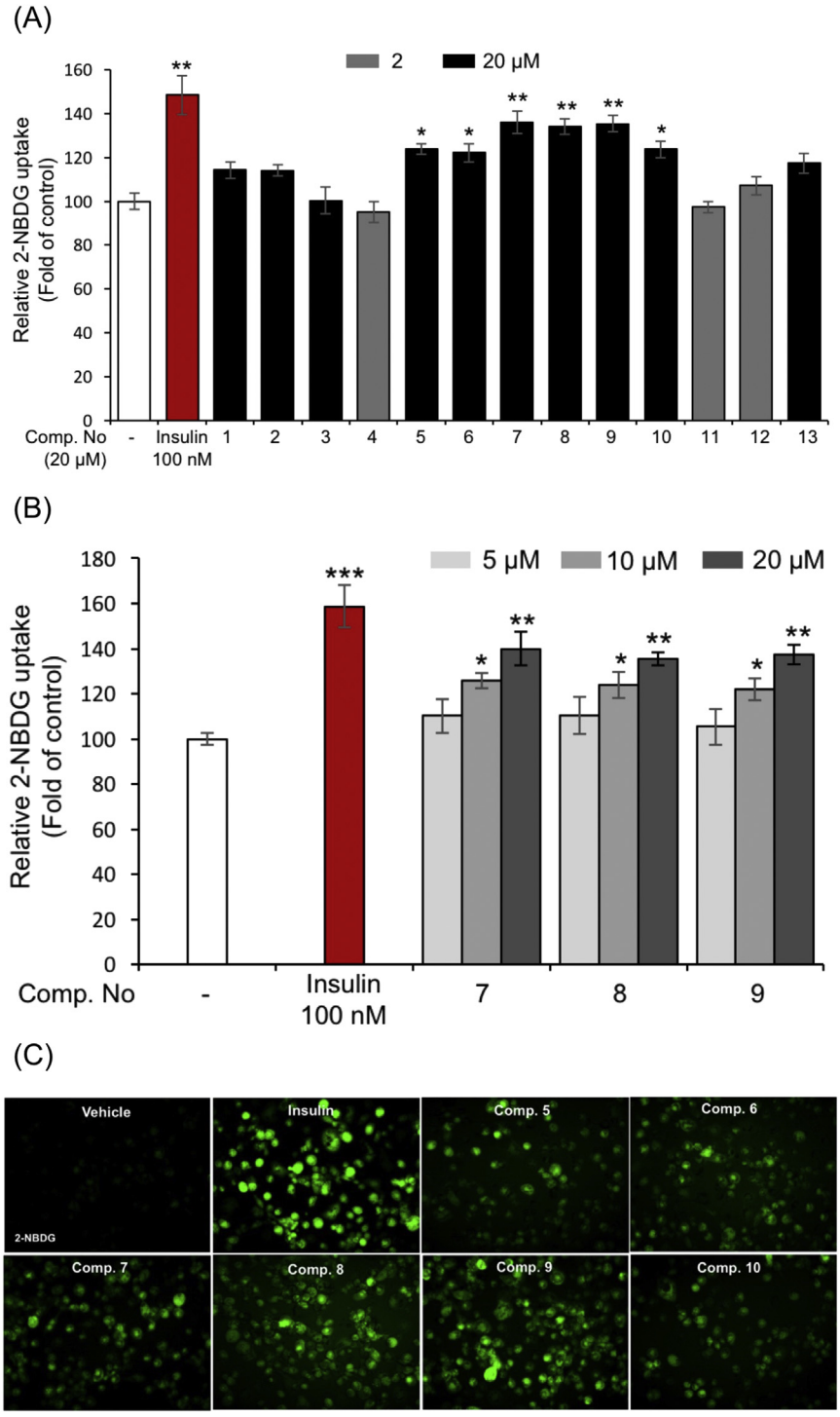

Fig. 4. Effects of compounds **1**–**13** on glucose uptake by 3T3-L1 adipocytes using a fluorescent derivative of glucose, 2-NBDG. (A) All isolated compounds were administered to cells at 20 or 2 μM, and insulin (100 nM) was used as a positive control. After 1 h of incubation with or without 2-NBDG, fluorescent signal intensities were measured at Ex/Em = 450/535 nm. The data were calculated as the means ± SDs ($n = 3$), $^{*}p < 0.05$ and $^{**}p < 0.01$, compared with the DMSO-only treatment group. (B) Differentiated 3T3-L1 adipocytes were exposed to compounds **7**–**9** at various concentrations (5, 10, and 20 μM) for 1 h. Green fluorescent signals were measured and expressed as the means ± SDs ($n = 3$); $^{*}p < 0.05$, $^{**}p < 0.01$, and $^{***}p < 0.001$, compared with the vehicle group. (C) Enhancement of glucose uptake by differentiated 3T3-L1 adipocytes was obtained with several compounds at 20 μM or insulin (100 nM), as demonstrated via fluorescence microscopy. Green fluorescence in the cells was significantly enhanced, indicating that 2-NBDG was transported into these cells.

3. Conclusions

Integrated approaches, including morphological and anatomical comparisons, sequence analysis of the ITS region, and chemical investigation, strongly suggested that *Gymnema sylvestre* originating from different geographic localities should be considered at least two varieties (Indian and Vietnamese origin). The aglycones of the isolates were identified as C-4 gem-dimethylated olenane-type

triterpenes, including myrtillogenic acid, chichipegenin, sitakisogenin, maniladiol, gymnemagenol, and 3β,16β,28-trihydroxyolean-12-en-29,22β-olide. Some of these aglycones are similar to those of the Chinese variety (Ye et al., 2001b), and none of these have been detected in plants of Indian origin. In addition, none of the isolates featured gymnemagenin or gymnestrogenin as the backbone, in contrast to isolates of Indian origin (Di Fabio et al., 2015; Fabio et al., 2014). Most bioactivity studies of *G. sylvestre* have used the Indian type, and this study provides the first demonstration of stimulatory effects of purified compounds from the Vietnamese *G. sylvestre* variety on 2-NBDG uptake by 3T3-L1 adipocyte cells. The results of this study demonstrate that the variety of *G. sylvestre* from Vietnam is also a promising herbal medicine for the treatment of glucose metabolism disorders with an insulin-mimetic action.

4. Experimental section

4.1. Plant material

Samples of two varieties of *G. sylvestre* originating from India (GS-I) and Vietnam (GS-V1 and GS-V2) were cultivated under the same conditions at two WHO Good-Agriculture-Practice (GAP)-certified farms in Nam Dinh (20°09′26.2″N 106°19′06.3″E) and Thai Nguyen provinces (21°52′47.5″N 105°44′35.7″E) in Vietnam. All the samples were collected in September 2016. Voucher specimens of GS-I, GS-V1 and GS-V2 were deposited in the Medicinal Herbarium of Hanoi University of Pharmacy with the accession numbers HNIP-2016.05, HNIP-2016.06 and HNIP-2016.07, respectively. Commercial samples of *G. sylvestre* originating from Guangxi, China (GS-C), were purchased in June 2017 and used in the hydrolysis experiment.

4.2. Morphological and anatomical analyses

An EZ4 Stereo Microscope (Leica, Germany) was used to analyze the characteristics of *G. sylvestre* (Retz.) R.Br. ex Sm. (Asclepiadaceae), including life form, stem, leaves, flowers, fruits and seeds. Photographs were obtained with a Canon SD4500IS or Canon EOS 60D + Canon 100 mm f2.8 IS Macro (Canon Inc., Japan). For anatomical analysis, cross sections of fresh mature stems and leaves were prepared using a rotatory microtome and double-stained with methylene blue and carmine red. A light microscope MBL200 (A.Krüss Optronic, Germany) connected to a Canon SD4500IS (Canon Inc., Japan) was used to visualize the results.

4.3. ITS1-5.8S-ITS2 sequence analysis

Total DNA was extracted from 200 mg of fresh plant leaves using a DNeasy Plant Mini Kit (QIAGEN, Germany) with some modifications. The internal transcribed spacer sequence was amplified with the forward primer ITS5 (5′-GGAAGTAAAAGTCGTAACAAGG-3′) and the reverse primer ITS4 (5′- TCCTCCGCTTATTGATATGC-3′), supplied by Bioneer Corporation (Korea), using a Mastercycler pro S (Eppendorf AG., Germany). The PCR products were purified using a purification kit from Thermo Fisher (USA), and sequencing was conducted by Macrogen Inc. (Seoul, Korea). The DNA sequences were compared to published sequences available in GenBank (National Institutes of Health) using the Basic Local Alignment Search Tool (Blast) (Altschul et al., 1990).

Geneious was used to align the internal transcribed spacer (ITS1-5.8S-ITS2) sequences of two samples of *Gymnema sylvestre* collected from different regions of Vietnam (*G. sylvestre* V1 and V2), one sample of Indian origin domesticated in Vietnam (GS-I), and 18 ITS sequences of five species, *G. sylvestre, G. latifolium, G. inodorum, G. yunnanense* and *Marsdenia tenacissima* (as an outgroup), obtained through a Blast analysis. Detailed information of the analysis samples and their alignment is provided in Table S2 and Fig. S5 (Supplementary data). Finally, Geneious DNA sequencing analysis software (version 8.1.8, Biomatters Ltd., New Zealand) was used to construct a neighbor-joining phylogenetic tree with resampling bootstrap values above 75% (expressed as percentages of 1000 replicates) (Kearse et al., 2012).

4.4. Extraction and isolation of 3β-glucuronide oleane-triterpenes

4.4.1. General experimental procedures

Optical rotation was measured on a JASCO P-2000 polarimeter (JASCO International Co. Ltd., Tokyo, Japan). IR data were recorded on a Nicolet 6700 FT-IR spectrometer (Thermo Electron Corp., Waltham, MA, USA). The NMR data were analyzed using an AVANCE 500 MHz spectrometer (Bruker, Germany), JNM-ECA 600-MHz spectrometer (Jeol, Japan) or AVANCE III 800 HD spectrometer coupled with a 5-mm CPTCI cryoprobe (Bruker, Germany). The HRESIMS values were determined using an Agilent Technologies 6130 Quadrupole LC/MS spectrometer equipped with an Agilent Technologies 1260 Infinity LC system (Agilent Technologies, Inc., Santa Clara, CA, USA) and INNO C18 column (4.6 × 150 mm, particle size of 5 μm, 12 nm, J.K. Shah & Company, Korea). Silica gel (particle size: 63–200 μm) and RP-C_{18} (particle size of 40–63 μm), which were purchased from Merck (Darmstadt, Germany), and Sephadex LH-20 from Sigma-Aldrich (St. Louis, MO, USA) were used for CC. Silica gel 60 F_{254} and RP-18 F_{254} TLC plates were obtained from Merck (Darmstadt, Germany). A Gilson HPLC purification system equipped with an Optima Pak C_{18} column (10 × 250 mm, particle size of 10 μm; RS Tech, Seoul, Korea) was used with a flow rate of 2 mL/min, and UV detection at 205 and 254 nm was performed.

4.4.2. Extraction and isolation process

The aerial parts of the Vietnamese *G. sylvestre* variety (10 kg) were powdered, sonicated with 60% EtOH, and filtered, and the solvent was evaporated in vacuo. The crude extract (1 kg) was suspended in 30% EtOH, absorbed on Diaion HP20 macroporous resin, and washed with 30% EtOH, 50% EtOH, 95% EtOH, and acetone through a sequential elution process. The 95% EtOH fraction (300 g) was subjected to silica gel column chromatography (15 × 45 cm; particle size of 63–200 μm) using *n*-hexane/EtOAc (gradient from 10:1 to 0:1) and then EtOAc/MeOH (gradient from 6:1 to 0:1) to yield eight fractions (A-G) based on the thin-layer chromatography profile. Fraction F was separated by reversed-phase silica gel column chromatography and eluted with MeOH/H_2O (v/v, from 2:3 to 1:0) to yield 10 sub-fractions (FI-FX). Subfraction FII (10.0 g) was re-chromatographed by silica gel CC (5 × 20 cm; particle size of 40–63 μm) and eluted with CH_2Cl_2/MeOH (v/v, gradient from 6:1 to 0:1) to yield three sub-fractions, FII.N1 to FII.N3. Fraction FII.N2 was applied in succession to Sephadex LH-20 (MeOH) and HPLC (Optima Pak C_{18}, MeCN/H_2O (v/v, 3:7), flow rate of 2 mL/min) to afford compounds **1** (22.5 mg), **2** (4.7 mg) and **13** (45.0 mg). Fraction FII.N3 was developed on a reversed phase silica gel chromatographic column eluted with MeCN/H_2O (v/v, from 1:5 to 1:0) to yield four subfractions (FII.N3.R1-4). Subfraction F.II.N3.R1 was purified by HPLC (Optima Pak C_{18}, MeCN/H_2O (v/v, 3:7), flow rate of 2 mL/min) to afford compounds **3** (12.0 mg) and **10** (18.1 mg). Subfraction F.II.N3.R3 was purified by HPLC (Optima Pak C_{18}, MeCN/H_2O (v/v, 8:25), flow rate of 2 mL/min) to afford compounds **5** (7.9 mg) and **6** (14.0 mg). Fraction F.II.N3.R4 was applied in succession to Sephadex LH-20 (MeOH) and HPLC (Optima Pak C_{18}, MeCN/H_2O (v/v, 7:20), flow rate of 2 mL/min) columns to afford compounds **7** (5.5 mg) and **9** (5.1 mg). Fraction FV was chromatographed by reversed-phase silica gel column chromatography and eluted with MeCN/H_2O (v/v,

from 2:5 to 1:0) to yield 10 subfractions (FV.R1-R10). Subfraction FV.R10 was purified by HPLC (Optima Pak C_{18}, MeCN/H_2O (v/v, 2:5), flow rate of 2 mL/min) to afford compound **12** (9.1 mg). Fraction F.V.R6 was applied in succession to Sephadex LH-20 (MeOH) and HPLC (Optima Pak C_{18}, MeCN/H_2O (v/v, 7:20), flow rate of 2 mL/min) columns to afford compounds **8** (6.1 mg) and **11** (17.0 mg). Compound **4** (5.0 mg) was purified from fraction FX by HPLC (Optima Pak C_{18}, MeCN/H_2O (v/v, 3:5), flow rate of 2 mL/min).

4.4.3. Characteristic data of previously undescribed compounds *1*–*9*

*4.4.3.1. Gymnemoside ND1 (**1**).* Amorphous powder; α_D^{25} -24.5^0 (*c* 0.2, MeOH); UV(MeOH) λ_{max} (log ε) 200 (3.09) nm, IRν_{max}: 3399, 2943, 1706, 1371, 1051, 1030 cm^{-1}. ^{13}C NMR Table 1; ^{1}H NMR Table 2; HRESIMS *m/z* 825.4315[M − H]$^-$ (calcd for $C_{42}H_{65}O_{16}$, 825.4278).

*4.4.3.2. Gymnemoside ND2 (**2**).* Amorphous powder; α_D^{25} -23.3^0 (*c* 0.2, MeOH); UV(MeOH) λ_{max} (log ε) 200 (3.01) nm, IRν_{max}: 3416, 2920, 1728, 1441, 1084, 1021 cm^{-1}; ^{13}C NMR Table 1; ^{1}H NMR Table 2; HRESIMS *m/z* 825.4297[M − H]$^-$ (calcd for $C_{42}H_{65}O_{16}$, 825.4278).

*4.4.3.3. Gymnemoside ND3 (**3**).* Amorphous powder; α_D^{25} -5.9^0 (c 0.2, MeOH); UV(MeOH) λ_{max} (log ε) 200 (3.01) nm, IRν_{max}: 3374, 2932, 1712, 1367, 1081, 1023 cm^{-1}; ^{13}C NMR Table 1; ^{1}H NMR Table 2; HRESIMS *m/z* 811.4521[M − H]$^-$ (calcd for $C_{42}H_{67}O_{15}$, 811.4485).

*4.4.3.4. Gymnemoside ND4 (**4**).* Amorphous powder; α_D^{25} -8.7^0 (*c* 0.2, MeOH); UV(MeOH) λ_{max} (log ε) 200 (3.17) nm, IRν_{max}: 3399, 2926, 1720, 1459, 1352, 1164, 1083, 1022 cm^{-1}; ^{13}C NMR Table 1; ^{1}H NMR Table 2; HRESIMS *m/z* 779.4625[M − H]$^-$ (calcd for $C_{42}H_{67}O_{13}$, 779.4582).

*4.4.3.5. Gymnemoside ND5 (**5**).* Amorphous powder; α_D^{25} -22.3^0 (*c* 0.2, MeOH); UV(MeOH) λ_{max} (log ε) 200 (3.12) nm, IRν_{max}: 3389, 2913, 1731, 1435, 1085, 1025 cm^{-1}; ^{13}C NMR Table 1; ^{1}H NMR Table 2; HRESIMS *m/z* 811.4526 [M − H]$^-$ (calcd for $C_{42}H_{67}O_{15}$, 811.4485).

*4.4.3.6. Gymnemoside ND6 (**6**).* Amorphous powder; α_D^{25} -15.7^0 (*c* 0.2, MeOH); UV(MeOH) λ_{max} (log ε) 200 (3.10) nm, IRν_{max}: 3399, 2926, 1720, 1455, 1083, 1032 cm^{-1}; ^{13}C NMR Table 1; ^{1}H NMR Table 2; HRESIMS *m/z* 649.3967 [M − H]$^-$ (calcd for $C_{36}H_{57}O_{10}$, 649.3957).

*4.4.3.7. Gymnemoside ND7 (**7**).* Amorphous powder; α_D^{25} -12.4^0 (*c* 0.2, MeOH); UV(MeOH) λ_{max} (log ε) 200 (3.05) nm, IRν_{max}: 3409, 2946, 1736, 1465, 1362, 1067, 1032 cm^{-1}; ^{13}C NMR Table 1; ^{1}H NMR Table 2; HRESIMS *m/z* 649.3985 [M − H]$^-$ (calcd for $C_{36}H_{57}O_{10}$, 649.3957).

*4.4.3.8. Gymnemoside ND8 (**8**).* Amorphous powder; α_D^{25} -2.4^0 (*c* 0.2, MeOH); UV(MeOH) λ_{max} (log ε) 200 (3.18), 230 (2.67) nm, IRν_{max}: 3374, 2933, 1716, 1446, 1380, 1095, 1020 cm^{-1}; ^{13}C NMR Table 1; ^{1}H NMR Table 2; HRESIMS *m/z* 769.4210 [M − H]$^-$ (calcd for $C_{43}H_{61}O_{12}$, 769.4169).

*4.4.3.9. Gymnemoside ND9 (**9**).* Amorphous powder; α_D^{25} -22.5^0 (*c* 0.2, MeOH); UV(MeOH) λ_{max} (log ε) 200 (3.15), IRν_{max}: 3414, 2953, 1706, 1350, 1051, 1005 cm^{-1};^{13}C NMR Table 1; ^{1}H NMR Table 2; HRESIMS *m/z* 661.3616 [M − H]$^-$ (calcd for $C_{36}H_{53}O_{11}$, 661.3593).

4.5. Acid hydrolysis

To perform acid hydrolysis, 2 mg of compound **1** or **2** was added to 1 mL of 5 M HCl in 60% ethanol, and the mixture was incubated at 90 °C for 24 h. The hydrolysis solutions were extracted with ethyl acetate, and the aqueous acid solution was evaporated to furnish the monosaccharide residue. The monosaccharides were identified as glucose and glucuronic acid in **1** and galactose and glucuronic acid in **2** by comparison with authentic samples by TLC in MeCOEt:iso-PrOH:acetone:H_2O (20:10:7:6); detection was accomplished with 20% H_2SO_4 and heating. The optical rotation of the purified sugars isolated from the hydrolysis product of fraction F revealed that the sugars were D-glucose, D-galactose, and D-glucuronic acid.

4.6. Differentiation of 3T3-L1 adipocytes

3T3-L1 fibroblasts were differentiated to 3T3-L1 adipocytes using DMEM (HyClone, UT, USA) containing 10% fetal bovine serum (FBS) (HyClone, UT, USA), 1 μM dexamethasone (Sigma, MO, USA), 520 μM 3-isobutyl-1-methyl-xanthine (Sigma, MO, USA) and 1 μg/mL insulin (Roche, Germany). The cells were continually incubated with fresh DMEM supplemented with 10% FBS, 1 μg/mL insulin, 100 U/mL penicillin and 100 μg/mL streptomycin (Gibco, NY, USA). The fresh medium was replaced every two days for four to six days until induction of adipogenesis.

4.7. Cytotoxicity assay

The 3T3-L1 adipocytes were seeded onto 96-well plates in DMEM supplemented with 10% FBS and incubated for one day. The cells were then exposed to compounds dissolved in serum-free media for 24 h. Cytotoxicity assays were subsequently performed using (3-(4,5-dimethyl-2-thiazolyl)-2,5-diphenyl-2H-tetrazolium bromide (MTT) (Sigma, MO, USA). In each well, 20 μL of 2 mg/mL MTT solution was added and incubated for 4 h at 37 °C in the dark. After removing the supernatant, the formazan was dissolved in 100 μL of DMSO, and the absorbance was measured at 550 nm using a microplate reader (VersaMax™, Radnor, PA, USA).

4.8. Measurement of glucose uptake levels

Glucose uptake assays were performed using a fluorescent derivative of glucose 2-[*N*-(7-nitrobenz-2-oxa-1,3-diazol-4-yl) amino]-2-deoxyglucose (2-NBDG) (Invitrogen, OR, USA) as previously described (Nguyen et al., 2017; Yang et al., 2017) with slight modifications. Briefly, 3T3-L1 adipocytes were seeded onto the 96-well plates in glucose-free media supplemented with 10% FBS. The glucose uptake assay was performed as follows: cells were treated with the test compounds or insulin as a positive control and incubated with or without 2-NBDG. The cultures were incubated for 1 h at 37 °C and 5% CO_2, and the cells were washed with cold phosphate-buffered saline (PBS). The fluorescent signal intensity was measured using Ex/Em wavelengths of 450/535 nm, respectively, with a fluorescence microplate reader (Spectra Max GEMINI XPS, Molecular Devices, CA, USA). To capture fluorescent images, 3T3-L1 adipocytes were grown on sterilized glass coverslips using glucose-free media, and the experimental procedures were performed as described above. After 1 h of incubation, the cells were washed with cold PBS, and images were obtained by fluorescence microscopy (Olympus ix70 Fluorescence Microscope, Olympus Corporation, Tokyo, Japan).

4.9. Statistical analysis

The data were calculated as the means ± SDs of three independent experiments. Differences between groups were determined by analysis of variance (ANOVA). Statistical significance was accepted at $^{*}p < 0.05$, $^{**}p < 0.01$, and $^{***}p < 0.001$.

Conflicts of interest

The authors declare no competing financial interest.

Acknowledgements

This work was financially supported in part by grants from the KBNMB (NRF-2017M3A9B8069409) and from the Basic Science Research Program (NRF-2017R1E1A1A01074674) through the National Research Foundation of Korea funded by the Ministry of Science, ICT & Planning. We would like to acknowledge Dr. Khuat Huu Trung of the Agricultural Genetic Institute, Vietnam, for his support in DNA sequencing and analysis.

Appendix A. Supplementary data

Supplementary data related to this article can be found at https://doi.org/10.1016/j.phytochem.2018.02.013.

References

Altschul, S.F., Gish, W., Miller, W., Myers, E.W., Lipman, D.J., 1990. Basic local alignment search tool. J. Mol. Biol. 215, 403–410. https://doi.org/10.1016/S0022-2836(05)80360-2.

Di Fabio, G., Romanucci, V., Di Marino, C., Pisanti, A., Zarrelli, A., 2015. Gymnema sylvestre R. Br., an Indian medicinal herb: traditional uses, chemical composition, and biological activity. Curr. Pharmaceut. Biotechnol. 16, 506–516.

Fabio, G.D., Romanucci, V., De Marco, A., Zarrelli, A., 2014. Triterpenoids from Gymnema sylvestre and their pharmacological activities. Molecules 19, 10956–10981. https://doi.org/10.3390/molecules190810956.

Frank, R.A., Mize, S.J.S., Kennedy, L.M., de los Santos, H.C., Green, S.J., 1992. The effect of Gymnema sylvestre extracts on the sweetness of eight sweeteners. Chem. Senses 17, 461–479. https://doi.org/10.1093/chemse/17.5.461.

Ge, Y.-W., Tohda, C., Zhu, S., He, Y.-M., Yoshimatsu, K., Komatsu, K., 2016. Effects of oleanane-type triterpene saponins from the leaves of eleutherococcus senticosus in an axonal outgrowth assay. J. Nat. Prod. 79, 1834–1841. https://doi.org/10.1021/acs.jnatprod.6b00329.

Gent, J.F., Hettinger, T.P., Frank, M.E., Marks, L.E., 1999. Taste confusions following gymnemic acid rinse. Chem. Senses 24, 393–403.

Kashima, H., Eguchi, K., Miyamoto, K., Fujimoto, M., Endo, M.Y., Aso-Someya, N., Kobayashi, T., Hayashi, N., Fukuba, Y., 2017. Suppression of oral sweet taste sensation with Gymnema sylvestre affects postprandial gastrointestinal blood flow and gastric emptying in humans. Chem. Senses 42, 295–302. https://doi.org/10.1093/chemse/bjw126.

Kearse, M., Moir, R., Wilson, A., Stones-Havas, S., Cheung, M., Sturrock, S., Buxton, S., Cooper, A., Markowitz, S., Duran, C., Thierer, T., Ashton, B., Meintjes, P., Drummond, A., 2012. Geneious Basic: an integrated and extendable desktop software platform for the organization and analysis of sequence data. Bioinformatics 28, 1647–1649. https://doi.org/10.1093/bioinformatics/bts199.

Lee, J., Jung, D.-W., Kim, W.-H., Um, J.-I., Yim, S.-H., Oh, W.K., Williams, D.R., 2013. Development of a highly visual, simple, and rapid test for the discovery of novel insulin mimetics in living vertebrates. ACS Chem. Biol. 8, 1803–1814. https://doi.org/10.1021/cb4000162.

Nguyen, P.H., Choi, H.S., Ha, T.K.Q., Seo, J.Y., Yang, J.L., Jung, D.-W., Williams, D.R., Oh, W.K., 2017. Anthraquinones from Morinda longissima and their insulin mimetic activities via AMP-activated protein kinase (AMPK) activation. Bioorg. Med. Chem. Lett 27, 40–44. https://doi.org/10.1016/j.bmcl.2016.11.034.

Pothuraju, R., Sharma, R.K., Chagalamarri, J., Jangra, S., Kumar Kavadi, P., 2014. A systematic review of Gymnema sylvestre in obesity and diabetes management. J. Sci. Food Agric. 94, 834–840. https://doi.org/10.1002/jsfa.6458.

Quijano, L., Rios, T., Fronczek, F.R., Fischer, N.H., 1998. The molecular structure of maniladiol from BacchariS salicina1In memory of Dr Lydia Rodrıguez-Hahn (1932–1998).1. Phytochemistry 49, 2065–2068. https://doi.org/10.1016/S0031-9422(98)00363-X.

Shobana, S., Kumari, S.R.U., Malleshi, N.G., Ali, S.Z., 2007. Glycemic response of rice, wheat and finger millet based diabetic food formulations in normoglycemic subjects. Int. J. Food Sci. Nutr. 58, 363–372. https://doi.org/10.1080/09637480701252229.

Tiwari, P., Mishra, B.N., Sangwan, N.S., 2014. Phytochemical and pharmacological properties of Gymnema sylvestre: an important medicinal plant. BioMed Res. Int. 2014 https://doi.org/10.1155/2014/830285, 830285–18.

Wang, Y., Feng, Y., Wang, X., Xu, H., 2004. Isolation and identification of a new component from Gymnema sylvestre. West China J. Pharm. Sci. 19, 336–338.

Warren, R.M., Pfaffmann, C., 1959. Suppression of sweet sensitivity by potassium gymnemate. J. Appl. Physiol. 14, 40–42.

White, T.J., Bruns, T., Lee, S., Taylor, J., 1990. Amplification and direct sequencing of fungal ribosomal rna genes for phylogenetics. In: PCR Protocols. Elsevier, pp. 315–322. https://doi.org/10.1016/B978-0-12-372180-8.50042-1.

Wu, Z.Y., Raven, P.H., 1995 (Gentianaceae through Boraginaceae). Flora of China, vol. 16. Science Press, Beijing, and Missouri Botanical Garden Press, St. Louis.

Yang, J.L., Ha, T.K.Q., Lee, B.W., Kim, J., Oh, W.K., 2017. PTP1B inhibitors from the seeds of Iris sanguinea and their insulin mimetic activities via AMPK and ACC phosphorylation. Bioorg. Med. Chem. Lett. https://doi.org/10.1016/j.bmcl.2017.09.031.

Ye, W., Liu, X., Zhang, Q., Che, C.T., Zhao, S., 2001a. Antisweet saponins from Gymnema sylvestre. J. Nat. Prod. 64, 232–235.

Ye, W.-C., Liu, X., Zhao, S.-X., Che, C.-T., 2001b. Triterpenes from Gymnema sylvestre growing in China. Biochem. Systemat. Ecol. 29, 1193–1195. https://doi.org/10.1016/S0305-1978(01)00060-6.

Ye, W.-C., Zhang, Q.-W., Liu, X., Che, C.-T., Zhao, S.-X., 2000. Oleanane saponins from Gymnema sylvestre. Phytochemistry 53, 893–899. https://doi.org/10.1016/S0031-9422(99)00483-5.

Yoshikawa, K., Ogata, H., Arihara, S., Chang, H.-C., Wang, J.-D., 1998. Antisweet natural products. Xiii. Structures of alternosides I-X from Gymnema alternifolium. Chem. Pharm. Bull. 46, 1102–1107. https://doi.org/10.1248/cpb.46.1102.

Yoshikawa, K., Takahashi, K., Matsuchika, K., Arihara, S., Chang, H.-C., Wang, J.-D., 1999. Antisweet natural products. Xiv. Structures of alternosides XI-XIX from Gymnema alternifolium. Chem. Pharm. Bull. 47, 1598–1603. https://doi.org/10.1248/cpb.47.1598.

Yoshikawa, K., Taninaka, H., Kan, Y., Arihara, S., 1994. Antisweet natural products. XI. Structures of sitakisosides VI-X from Stephanotis lutchuensis Koidz. var. japonica. Chem. Pharm. Bull. 42, 2455–2460.

Zhao, J.-Q., Wang, Y.-M., Yang, Y.-L., Zeng, Y., Mei, L.-J., Shi, Y.-P., Tao, Y.-D., 2017. Antioxidants and α -glucosidase inhibitors from “Liucha” (young leaves and shoots of Sibiraea laevigata). Food Chem. 230, 117–124. https://doi.org/10.1016/j.foodchem.2017.03.024.